

电针患侧曲池、阳陵泉穴对脑梗死后肢体痉挛大鼠的影响与机制研究

绽 晟, 黄麟荇, 易丽贞, 陈瑞雪, 黄慧源, 岳增辉*

湖南中医药大学针灸推拿与康复学院, 湖南 长沙 410208

*通信作者: 岳增辉, E-mail: 624755064@qq.com

收稿日期: 2023-11-05; 接受日期: 2024-01-21

基金项目: 国家自然科学基金项目(81673886); 湖南省自然科学基金项目(2023JJ30462);

湖南省研究生创新课题(CX20220797)

DOI: 10.3724/SP.J.1329.2024.02006

开放科学(资源服务)标识码(OSID): [https://doi.org/10.3724/SP.J.1329.2024.02006](#)



摘要 目的 观察电针患侧曲池、阳陵泉穴对脑梗死后肢体痉挛(PSS)大鼠皮质损伤及血清炎性因子[白细胞介素-6(IL-6)、肿瘤坏死因子- α (TNF- α)]、谷氨酸(Glu)、丙二醛(MDA)、核黄素激酶(RFK)和还原性辅酶氧化酶2(NOX2)表达的影响,探讨电针治疗缺血性脑卒中后脑损伤的机制。**方法** 选择SPF级健康成年SD雄性大鼠30只,采用随机数字表法分为假手术组与造模组,每组10、20只。造模组采用Zea-Longa线栓法联合内囊注射N-甲基-D-天冬氨酸(NMDA)制备PSS大鼠模型。造模成功后,造模组按随机数字表法分为模型组、电针组,每组10只。模型组采用鼠板固定大鼠,但不进行干预;电针组接受电针干预,穴位选择患侧阳陵泉穴(左)、曲池穴(左),每穴直刺1针,电针波型:密波;频率:100 Hz,强度以大鼠肢体轻微抖动为度,30 min/次,1次/d,连续治疗7 d。分别于造模第1天和治疗第7天采用Zea-Longa神经功能评分评估大鼠神经功能受损程度;分别于造模第2天和治疗第7天采用改良Ashworth量表(MAS)评分评估大鼠患侧肢体肌张力;采用HE染色观察大脑皮质的病理学改变;行为学测试完毕后,采用酶联免疫吸附法(ELISA法)检测MDA、Glu含量和大脑皮质中IL-6、TNF- α 含量;采用Western blot法分析RFK、NOX2蛋白表达水平;采用RT-PCR法分析RFK、NOX2 mRNA转录水平。**结果** ① Zea-Longa神经功能、MAS评分:与治疗前比较,电针组治疗后Zea-Longa神经功能、MAS评分均明显降低($P<0.05$)。与假手术组比较,模型组、电针组治疗前Zea-Longa神经功能、MAS评分均明显升高($P<0.05$);与模型组比较,电针组治疗后Zea-Longa神经功能、MAS评分均明显降低($P<0.05$)。② 脑组织病理学改变:模型组可见脑组织水肿,胞核深染,形态不规则、固缩、空泡变性,炎性细胞浸润等病理学改变;与模型组比较,电针组脑组织病变改善,神经元损伤程度减轻,可见较多正常细胞,细胞轮廓清晰,炎性细胞数量减少。③ 缺血侧皮质TNF- α 、IL-6、Glu、MDA含量:与假手术组比较,模型组、电针组TNF- α 、IL-6、Glu、MDA含量明显升高($P<0.05$);与模型组比较,电针组TNF- α 、IL-6、Glu、MDA含量明显降低($P<0.05$)。④ RFK、NOX2蛋白表达水平和RFK、NOX2 mRNA转录水平:与假手术组比较,模型组RFK、NOX2蛋白表达水平和RFK、NOX2 mRNA转录水平明显升高($P<0.05$);与模型组比较,电针组干预后RFK、NOX2蛋白表达水平和RFK、NOX2 mRNA转录水平明显降低($P<0.05$)。**结论** 电针可以改善PSS大鼠神经功能损伤和肢体痉挛状态,其作用机制可能与下调皮质Glu含量,减少炎性因子TNF- α 、IL-6分泌,抑制RFK、NOX2表达,降低氧化应激水平有关。

关键词 脑梗死; 肢体痉挛; 神经功能障碍; 氧化应激; 电针; 曲池穴; 阳陵泉穴

引用格式: 绛晟, 黄麟荇, 易丽贞, 等. 电针患侧曲池、阳陵泉穴对脑梗死后肢体痉挛大鼠的影响与机制研究[J]. 康复学报, 2024, 34(2):133-139.

ZHAN S, HUANG L X, YI L Z, et al. Effect and mechanism of electroacupuncture at the affected side of Quchi (LI 11) and Yanglingquan (GB 34) acupoints in rats with limb spasms after cerebral infarction [J]. Rehabil Med, 2024, 34(2):133-139.

DOI: 10.3724/SP.J.1329.2024.02006

脑卒中肢体痉挛(post-stroke spasticity, PSS)是脑卒中患者最常见的肢体功能障碍,具有较高的发病率、致残率^[1]。脑缺血发生后,脑组织在缺血环境下释放炎症因子,促进产生大量活性氧(reactive oxygen species, ROS),加强氧化应激最终影响患者预后^[2]。中枢神经系统中的ROS主要来源于还原型烟酰胺腺嘌呤二核苷酸磷酸(reduced nicotinamide adenine dinucleotide phosphate, NAPDH)氧化酶2(oxidase 2, NOX2),是病理条件下引起氧化应激的主要来源^[3]。NOX2是一种多亚单位蛋白质复合体,通过将电子从胞内NADPH转移到分子氧产生过氧化氢、超氧化物和羟自由基在内的活性氧,导致机体氧化和抗氧化系统失衡,引起组织损伤^[4-5]。核黄素激酶(riboflavin kinase, RFK)是催化黄素单核苷酸(flavin mononucleotide, FMN)辅因子生物合成的重要酶,其与肿瘤坏死因子受体的结合可以增强NOX2对ROS的生成。ROS在大多数情况下作为重要代谢途径的副产品生成,很难从源头抑制ROS生成。因此,抑制NOX2抵抗组织中氧化应激可能是降低脑梗死后脑组织神经损伤的重要方式^[6]。

本项目组前期研究证实了电针“曲池”“阳陵泉”对缺血性脑卒中大鼠的神经修复功能^[7-10],但对脑卒中后氧化应激状态的影响及其机制尚不明确。本研究利用线栓结合内囊注射N-甲基-D-天冬氨酸(N-methyl-D-aspartate, NMDA)受体法构建大鼠PSS模型,并予电针干预,探讨电针对脑梗死后大鼠皮质炎性因子、氧化应激相关蛋白表达的影响及其作用机制,为电针干预脑梗死后肢体痉挛状态提供理论依据。

1 材料与方法

1.1 实验动物选择

选择SPF级健康成年SD雄性大鼠30只,2~3月龄,体质量(280 ± 20)g,购自湖南斯莱克景达实验动物有限公司,实验动物生产许可证号:SCXK(湘)2019-0004。于湖南中医药大学动物中心分笼饲养,普通饲料投喂,室温(25 ± 2)℃,相对湿度65%~70%,自然光照,自由进食饮水。

1.2 主要试剂与仪器

NMDA受体(美国Sigma公司);戊巴比妥钠(中国医药集团有限公司);线栓(北京西浓科技有限公司);脑立体定位仪(日本成茂公司,型号:SN-2);牙科钻(南京金恒川电子有限公司);透射电子显微镜(日本Hitachi公司,型号:HT7800/HT7700);丙二醛

(malondialdehyde, MDA)含量试剂盒(长沙雅尔贸易有限公司);亚铁含量(亚铁嗪比色法)检测试剂盒(长沙雅尔贸易有限公司);谷胱甘肽(glutathione, GSH)-ELISA检测试剂盒(厦门仑昌硕生物科技有限公司);GSH抗体(北京博奥森生物技术有限公司,货号:bs-11612R);Trizol试剂(美国英杰生命技术有限公司,货号:10296028);荧光定量PCR仪(美国Applied Biosystems公司,型号:StepOne Software);电泳仪(北京百晶生物技术有限公司,型号:BG-subMIDI);针灸针(苏州医疗用品厂有限公司,规格:0.25 mm×15 mm);电针仪(苏州医疗用品厂有限公司,型号:SDZ-V)。

1.3 实验动物模型制备与分组

1.3.1 实验动物模型制备 将SD大鼠适应性喂养7 d后,采用随机数字表法分为假手术组与造模组,每组10、20只。造模组采用Zea-Longa线栓法联合内囊注射NMDA法制备PSS大鼠模型^[11-12]。

1.3.1.1 Zea-Longa线栓法 第1天,大鼠腹腔注射2%戊巴比妥钠(50 mg/kg)麻醉后仰卧固定,剃毛备皮后碘伏消毒,沿大鼠的颈正中线偏右侧方切口,充分暴露右侧颈总动脉(common carotid artery, CCA)和迷走神经,继续向上分离至CCA分叉处,将颈内动脉(internal carotid artery, ICA)与颈外动脉(external carotid artery, ECA)分离,将CCA、ECA近心端结扎,将ICA夹闭,在CCA分叉膨大5 mm处用眼科剪剪一小切口,将线栓沿切口插入,松开ICA,线栓经CCA插入ICA,稍感阻力时停止插入线栓(约18~20 mm),将ICA近心端与线栓结扎固定后缝合切口。大鼠苏醒后进行Zea-Longa评分,1~3分大鼠于第2天行内囊注射NMDA。

1.3.1.2 内囊注射NMDA受体 第2天,将大鼠麻醉后固定于脑立体定位仪上,沿颅顶正中切开约2 cm,逐层分离,充分暴露前、后囟,根据《大鼠脑立体定位图谱》^[13]确定内囊位置后在前囟后1.4 mm、矢状缝右2.4 mm钻孔,将微量注射器插入7 mm,以1 μL/min速度注射5 μL NMDA,注射完毕留针8~10 min,出针后棉球按压止血后缝合切口。大鼠麻醉苏醒后,将Zea-Longa神经功能缺损评分为1~3分,改良Ashworth肌张力评分为1~4分视为造模成功^[14]。

1.3.2 实验动物分组 造模成功后,造模组按随机数字表法分为模型组、电针组,每组10只。本实验方案通过湖南中医药大学实验动物伦理委员会审批(审批号:LL2022031601)。

1.4 干预方法

1.4.1 假手术组 第1天仅分离血管不插线栓,第2天脑立体定位后注射等量0.9%NaCl溶液,不进行干预。

1.4.2 模型组 采用鼠板固定大鼠,但不进行干预。

1.4.3 电针组 电针组接受电针干预。首先,采用鼠板固定大鼠,一次性针灸针针刺患侧阳陵泉穴(左)、曲池穴(左),每穴直刺1针。然后,连接SDZ-V电针治疗仪,将针灸针连接电极,波型:密波;频率:100 Hz;强度以大鼠肢体轻微抖动为度。30 min/次,1次/d,连续干预7 d。

1.5 观察指标

1.5.1 神经功能损伤 分别于造模第1天和治疗第7天采用Zea-Longa神经功能评分^[14]评估大鼠神经功能受损程度。评分共5级,分值越高,提示神经功能受损越严重。

1.5.2 肌张力 分别于造模第2天和治疗第7天采用改良Ashworth量表(modified Ashworth scale,MAS)评分评估大鼠患侧肢体肌张力^[15]。共分为6级:0、1、1⁺、2、3、4,分别记为0~5分。分值越高,提示肌肉痉挛程度越高。

1.5.3 脑组织病理学改变 行为学测试完毕后,大鼠腹腔内注射2%戊巴比妥钠(50 mg/kg)深度麻醉,0.9% NaCl溶液和4%多聚甲醛溶液经心内灌注进行组织固定,冰上迅速剥离缺血侧皮质,取一半放在10%福尔马林缓冲液中固定48 h,再进行常规石蜡包埋,石蜡包埋的组织切片厚度约为5 μm,HE染色,于显微镜400倍视野下拍照。HE染色观察大脑皮质的病理学改变。

1.5.4 MDA、谷氨酸含量和血清炎症因子 称取100 mg缺血侧皮质组织,加入1 mL提取液进行冰浴匀浆;8 000×g 4 ℃离心10 min,取上清,严格按照生化试剂盒说明书步骤操作检测MDA、谷氨酸(glutamic acid,Glu)含量;按照ELISA试剂盒说明步骤检测大脑皮质中白细胞介素-6(interleukin,IL-6)、肿瘤坏死因子-α(tumor necrosis factor-α,TNF-α)含量。

1.5.5 缺血侧皮质RFK、NOX2蛋白表达水平 每组随机选取3只大鼠,麻醉后断头取脑,冰上取患侧大脑皮质20 mg。提取蛋白后采用BCA法测定蛋白浓度,制备凝胶,电泳,转膜后置于封闭液中封闭,依次孵育一抗、二抗后置于暗室ECL显影,以β-actin为内参,采用Western blot法分析平均灰度值的比值作为蛋白质相对表达量。

1.5.6 缺血侧皮质RFK、NOX2蛋白mRNA转录水

平 每组随机选取3只大鼠,按上述步骤取大脑皮质20 mg。使用TriZol法提取总RNA后测mRNA浓度,并计算加样量。逆转录cDNA,循环后以β-actin为内参,采用RT-PCR法($2^{-\Delta\Delta C_t}$)分析RFK、NOX2 mRNA转录水平。目标基因引物序列见表1。

表1 目标基因引物序列

Table1 Primer sequence of target gene

基因名称	引物序列
NOX2	正向:ACGCACCCTTCAAAACCATC 反向:AATGGGTGCCACTCTAGCTTG
RFK	正向:CGTTCTCTGCGAGGTCA 反向:GCCAGCCGTAATAGATGC
β-actin	正向:CTGAACGTGAAATTGTCCGAGA 反向:TTGCCAATGGTGATGACCTG

1.6 统计学方法

采用SPSS 25.0统计软件进行数据分析。计量资料服从正态分布以($\bar{x}\pm s$)表示,多组间比较采用单因素方差分析,组间两两比较采用Bonferroni检验;不满足正态分布以 $M(P_{25},P_{75})$ 表示,组内比较采用配对秩和检验,组间比较采用Kruskal-Wallis H检验。 $P<0.05$ 为差异具有统计学意义。

2 结 果

2.1 3组大鼠神经功能缺损评分比较

与治疗前比较,电针组治疗后Zea-Longa神经功能评分明显降低($P<0.05$)。与假手术组比较,模型组、电针组治疗前Zea-Longa神经功能评分明显升高($P<0.05$);与模型组比较,电针组治疗后Zea-Longa神经功能评分明显降低($P<0.05$)。见表2。

表2 3组治疗前后Zea-Longa神经功能

评分比较[$M(P_{25},P_{75})$]

分

Table 2 Comparison of Zea-Longa neurological function score in three groups before and after treatment [$M(P_{25},P_{75})$] Scores

组别	n	治疗前	治疗后	Scores
假手术组	10	0(0,0)	0(0,0)	
模型组	10	3(2,3) ¹⁾	2(2,3)	
电针组	10	3(2,3) ¹⁾	1(1,2) ²⁾³⁾	

注:与假手术组比较,1) $P<0.05$;与模型组比较,2) $P<0.05$;
与治疗前比较,3) $P<0.05$ 。

Note: Compared with the sham operation group, 1) $P<0.05$; compared with the model group, 2) $P<0.05$; compared with that before treatment, 3) $P<0.05$.

2.2 3组 MAS 评分比较

与治疗前比较,电针组治疗后 MAS 评分明显降低($P<0.05$)。与假手术组比较,模型组、电针组治疗前 MAS 评分明显升高($P<0.05$);与模型组比较,电针组治疗后 MAS 评分明显降低($P<0.05$)。见表 3。

2.3 3组 脑组织病理学改变

假手术组脑组织形态和结构未见异常;模型组可见脑组织水肿,胞核深染,形态不规则、固缩、空泡变性,炎性细胞浸润等病理学改变;与模型组比较,电针组脑组织神经元损伤程度减轻,可见较多正常细胞,细胞轮廓清晰,炎性细胞数量减少。见图 1。

2.4 3组 MDA、Glu 含量和血清 IL-6、TNF- α 比较

与假手术组比较,模型组、电针组 MDA、Glu 含

量和血清 IL-6、TNF- α 明显升高($P<0.05$);与模型组比较,电针组 MDA、Glu 含量和血清 IL-6、TNF- α 含量明显降低($P<0.05$)。见表 4。

表 3 3组治疗前后 MAS 评分比较 [$M(P_{25}, P_{75})$] 分
Table 3 Comparison of MAS score in three groups before and after treatment [$M(P_{25}, P_{75})$] Scores

组别	n	治疗前	治疗后
假手术组	10	0(0,0)	0(0,0)
模型组	10	3(2.75,4) ¹⁾	3(2,3)
电针组	10	3(2,3.25) ¹⁾	1(1,2) ²⁽³⁾

注:与假手术组比较,1) $P<0.05$;与模型组比较,2) $P<0.05$;与治疗前比较,3) $P<0.05$ 。

Note: Compared with the sham operation group, 1) $P<0.05$; compared with the model group, 2) $P<0.05$; compared with that before treatment, 3) $P<0.05$.

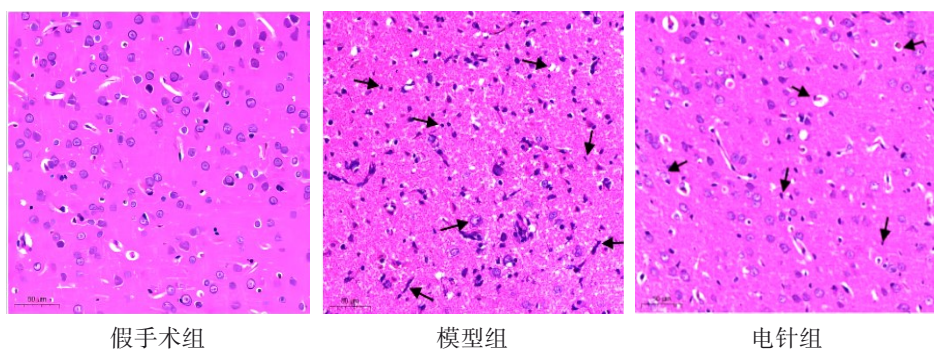


图 1 3组大脑皮质病理学形态 HE 染色图($\times 400$)

Figure 1 HE staining of pathological morphology of cerebral cortex in three groups ($\times 400$)

表 4 3组 MDA、Glu 含量和血清 IL-6、TNF- α 比较($\bar{x}\pm s$)

Table 4 Comparison of MDA, Glu and IL-6, TNF- α of serum in three group ($\bar{x}\pm s$)

组别	n	MDA/(nmol/g)	Glu/(\mu mol/mL)	血清 IL-6/(pg/mL)	血清 TNF- α /(pg/mL)
假手术组	10	1 390.19 \pm 440.15	1 808.456 \pm 727.912	375.961 \pm 97.507	1 230.806 \pm 186.151
模型组	10	5 149.27 \pm 876.91 ¹⁾	7 995.974 \pm 1 020.732 ¹⁾	1 510.105 \pm 230.560 ¹⁾	3 744.191 \pm 314.680 ¹⁾
电针组	10	3 093.05 \pm 768.67 ¹⁽²⁾	3 789.738 \pm 1 544.320 ¹⁽²⁾	857.603 \pm 249.678 ¹⁽²⁾	1 934.892 \pm 607.904 ¹⁽²⁾

注:与假手术组比较,1) $P<0.05$;与模型组比较,2) $P<0.05$ 。

Note: Compared with the sham operation group, 1) $P<0.05$; compared with the model group, 2) $P<0.05$.

2.5 3组缺血侧皮质 RFK、NOX2 蛋白表达水平比较

与假手术组比较,模型组 RFK、NOX2 表达水平明显升高($P<0.05$);与模型组比较,电针组 RFK、NOX2 蛋白表达水平明显降低($P<0.05$)。见图 2、表 5。

2.6 3组缺血侧皮质 RFK、NOX2 mRNA 转录水平比较

与假手术组比较,模型组 RFK、NOX2 mRNA 转录水平明显升高($P<0.05$);与模型组比较,电针组 RFK、NOX2 mRNA 转录水平明显降低($P<0.05$)。见表 6。

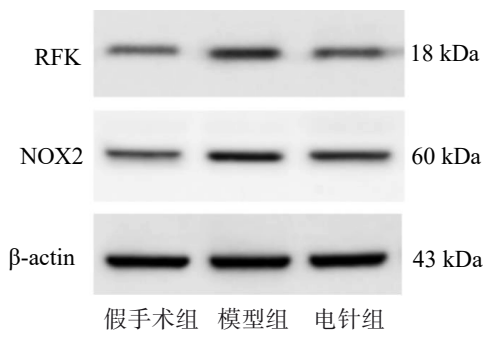


图2 3组RFK、NOX2蛋白条带图
Figure 2 Protein bands figure of RFK and NOX2 in three groups

表5 3组RFK、NOX2蛋白表达水平比较($\bar{x}\pm s$)

Table 5 Comparison of protein expression level of RFK and NOX2 in three groups ($\bar{x}\pm s$)

组别	n	RFK	NOX2
假手术组	3	0.18±0.01	0.41±0.02
模型组	3	0.33±0.01 ¹⁾	0.66±0.03 ¹⁾
电针组	3	0.27±0.02 ¹⁽²⁾	0.55±0.04 ¹⁽²⁾

注:与假手术组比较,1) $P<0.05$;与模型组比较,2) $P<0.05$ 。

Note: Compared with the sham operation group, 1) $P<0.05$; compared with the model group, 2) $P<0.05$.

表6 3组RFK、NOX2 mRNA表达水平比较($\bar{x}\pm s$)

Table 6 Comparison of mRNA expression level of RFK and NOX2 in three groups ($\bar{x}\pm s$)

组别	n	RFK	NOX2
假手术组	3	1.12±0.55	1.08±0.52
模型组	3	3.59±1.21 ¹⁾	5.87±1.16 ¹⁾
电针组	3	1.43±0.35 ¹⁽²⁾	2.67±1.09 ¹⁽²⁾

注:与假手术组比较,1) $P<0.05$;与模型组比较,2) $P<0.05$ 。

Note: Compared with the sham operation group, 1) $P<0.05$; compared with the model group, 2) $P<0.05$.

3 讨 论

3.1 电针曲池、阳陵泉穴可有效改善PSS大鼠神经功能和患侧肢体肌张力

本研究结果显示,与模型组比较,电针组治疗后Zea-Longa神经功能评分、MAS评分和Glu含量均明显降低,脑组织神经元损伤程度减轻,可见较多正常细胞,细胞轮廓清晰,炎性细胞数量减少,提示电针曲池、阳陵泉穴可有效改善PSS大鼠神经功能和患侧肢体肌张力。可能与以下原因有关:脑缺血后的病理变化可能导致膜电位去极化,兴奋性氨基酸尤其是Glu过量释放^[16]。突触间隙内Glu含量上

升并维持在较高水平,直接对神经元产生毒性作用。电针曲池、阳陵泉穴可以降低大脑皮质中Glu表达,抑制了Glu介导神经递质,降低脊髓前角运动神经元兴奋性毒性从而减轻神经元损伤,起到缓解痉挛的作用。曲池穴位于肘关节部位,阳陵泉穴居膝关节近处,二穴都在多气多血之阳明经脉上,上下配合,可以开四关、调气血、强筋骨,在电针的持续刺激下可促进肢体神经功能恢复,降低患侧肢体肌张力。

3.2 电针改善PSS大鼠神经功能和肢体痉挛状态可能与抑制炎症因子和RFK、NOX2蛋白表达相关

本研究结果显示,与模型组比较,电针组大鼠皮质炎性因子浸润明显降低,血清IL-6、TNF- α 与MDA含量下降,RFK、NOX2蛋白表达水平和RFK、NOX2 mRNA转录水平明显降低,提示电针改善PSS大鼠神经功能和肢体痉挛状态可能与抑制炎症因子和RFK、NOX2蛋白表达相关。可能与以下因素有关:①脑梗死发生后,缺血环境刺激小胶质细胞活化,引起TNF- α 、IL-6等促炎因子释放,炎症反应加重进而加快了神经元凋亡^[17]。电针曲池、阳陵泉穴可以抑制炎性因子浸润,抑制IL-6、TNF- α 释放,改善脑神经元损伤程度。TNF- α 已被证明可通过自身结构域与RFK结合,激活RFK过表达,启动NOX2^[18],产生大量ROS引起脂质过氧化。②脑组织富含不饱和脂肪酸与胆固醇,容易受到氧自由基的攻击,脂质过氧化物MDA是常用的氧化应激水平标志物。电针曲池、阳陵泉穴可以抑制TNF- α 介导的RFK与NOX2表达,降低脑损伤后MDA含量,调节脑损伤后脑内氧化应激水平,改善脑梗死大鼠神经功能。这与张立^[19]研究结果发现抑制NOX2可以有效缓解蛛网膜下腔出血后的一系列脑神经损伤的观点相似。

4 小 结

电针曲池、阳陵泉穴可以有效改善脑梗死后大鼠神经功能和肢体痉挛状态,其机制可能与下调皮质Glu含量,减少炎症因子TNF- α 、IL-6分泌,抑制RFK、NOX2表达,降低氧化应激水平有关。但NOX2、RFK只是氧化应激系统中的部分关键因子,并未从氧化应激系统深入讨论电针干预脑梗死后大鼠脑损伤机制,下一步仍需进一步从分子生物学和氧化应激反应层面进行深入研究,以期为电针干预脑梗死后神经功能障碍和肢体痉挛提供更多理论依据。

参考文献

- [1] WISSEL J, MANACK A, BRAININ M. Toward an epidemiology of poststroke spasticity [J]. Neurology, 2013, 80(3 Suppl 2):S13–S19.
- [2] WU M M, GU X P, MA Z L. Mitochondrial quality control in cerebral ischemia-reperfusion injury [J]. Mol Neurobiol, 2021, 58(10): 5253–5271.
- [3] BEGUM R, THOTA S, ABDULKADIR A, et al. NADPH oxidase family proteins: signaling dynamics to disease management [J]. Cell Mol Immunol, 2022, 19(6):660–686.
- [4] SAJJA R K, KAISAR M A, VIJAY V, et al. *In vitro* modulation of redox and metabolism interplay at the brain vascular endothelium: genomic and proteomic profiles of sulforaphane activity [J]. Sci Rep, 2018, 8(1):12708.
- [5] ZHAO Y L, XU J F. Sanggenon C ameliorates cerebral ischemia-reperfusion injury by inhibiting inflammation and oxidative stress through regulating RhoA-ROCK signaling [J]. Inflammation, 2020, 43(4):1476–1487.
- [6] ZHANG M R, CHEN H Q, ZHANG W L, et al. Biomimetic remodeling of microglial riboflavin metabolism ameliorates cognitive impairment by modulating neuroinflammation [J]. Adv Sci, 2023, 10(12):e2300180.
- [7] 岳增辉, 陈乐乐, 朱小娜, 等. 针刺对脑卒中痉挛大鼠模型大脑皮质DRD1 mRNA、DRD2 mRNA表达的影响[J]. 湖南中医药大学学报, 2012, 32(12):51–54.
- YUE Z H, CHEN L L, ZHU X S, et al. Effect of acupuncture on the dopamine receptors expression of DRD1 mRNA/DRD2 mRNA in cerebral cortex of spasticity model rats after stroke [J]. J Tradit Chin Med Univ Hunan, 2012, 32(12):51–54.
- [8] 郭斌, 岳增辉, 谢志强, 等. 基于神经兴奋-抑制因子(Glu-GABA)受体含量及表达观察电针对脑卒中痉挛状态大鼠黑质纹状体的影响实验研究[J]. 时珍国医国药, 2020, 31(5): 1268–1270.
- GUO B, YUE Z H, XIE Z Q, et al. Experimental study on the effect of electroacupuncture on substantia nigra striatum in spastic rats after stroke based on the content and expression of Glu-GABA receptor [J]. Lishizhen Med Mater Med Res, 2020, 31(5): 1268–1270.
- [9] 郭斌, 岳增辉, 谢志强, 等. 基于大脑黑质纹状体内多巴胺受体亚型含量与表达观察针刺对大鼠脑卒中痉挛状态的影响[J]. 中华中医药杂志, 2019, 34(2):577–579.
- GUO B, YUE Z H, XIE Z Q, et al. Effects of acupuncture on rats with SCA based on the quantity and expression of dopamine receptor subtypes in the brain substantia nigra corpus striatum [J]. Chin J Tradit Chin Med Pharm, 2019, 34(2):577–579.
- [10] 郭斌, 岳增辉, 谢志强, 等. 电针对脑卒中痉挛状态大鼠大脑皮质中谷氨酸与γ-氨基丁酸二者受体表达的影响[J]. 中华中医药杂志, 2019, 34(1):325–327.
- GUO B, YUE Z H, XIE Z Q, et al. Effects of electro-acupuncture on the expression of receptors of Glu and GABA in the cerebral cortex of rats with SCA [J]. Chin J Tradit Chin Med Pharm, 2019, 34(1):325–327.
- [11] MA J Y, ZHAO L, JR NOWAK T S. Selective, reversible occlusion of the middle cerebral artery in rats by an intraluminal approach. Optimized filament design and methodology [J]. J Neurosci Methods, 2006, 156(1/2):76–83.
- [12] 谢志强, 谢莉娜, 郭斌, 等. 脑卒中后肢体痉挛大鼠模型制备方法[J]. 中国中医药现代远程教育, 2019, 17(5):103–105.
- XIE Z Q, XIE L N, GUO B, et al. Methods of rat model preparation for limb spasm after stroke [J]. Chin Med Mod Distance Educ Chin, 2019, 17(5):103–105.
- [13] PAXINOS G W C. 大鼠脑立体定位图谱[M]. 3 版. 诸葛启钏,译. 北京:人民卫生出版社, 2005:44–45.
- PAXINOS G W C. The rat brain in stereotaxic coordinates [M]. 3rd Ed. ZHU-GE Q C, Translate. Beijing: People's Health Publishing House, 2005:44–45.
- [14] LONGA E Z, WEINSTEIN P R, CARLSON S, et al. Reversible middle cerebral artery occlusion without craniectomy in rats [J]. Stroke, 1989, 20(1):84–91.
- [15] BOHANNON R W, SMITH M B. Interrater reliability of a modified Ashworth scale of muscle spasticity [J]. Phys Ther, 1987, 67(2):206–207.
- [16] MERELLI A, REPETTO M, LAZAROWSKI A, et al. Hypoxia, oxidative stress, and inflammation: three faces of neurodegenerative diseases [J]. J Alzheimers Dis, 2021, 82(S1):S109–S126.
- [17] HE R Y, JIANG Y B, SHI Y J, et al. Curcumin-laden exosomes target ischemic brain tissue and alleviate cerebral ischemia-reperfusion injury by inhibiting ROS-mediated mitochondrial apoptosis [J]. Mater Sci Eng C Mater Biol Appl, 2020, 117:111314.
- [18] YAZDANPANAH B, WIEGMANN K, TCHIKOV V, et al. Riboflavin kinase couples TNF receptor 1 to NADPH oxidase [J]. Nature, 2009, 460(7259):1159–1163.
- [19] 张立. NADPH 氧化酶 NOX2/NOX4 在大鼠蛛网膜下腔出血后早期脑损伤中的作用及机制研究[D]. 苏州:苏州大学, 2017: 41–43.
- ZHANG L. The role of NOX2/NOX4 on early brain injury after experimental subarachnoid hemorrhage and its mechanism research [D]. Suzhou:Soochow University, 2017;41–43.

Effect and Mechanism of Electroacupuncture at the Affected Side of Quchi (LI 11) and Yanglingquan (GB 34) Acupoints in Rats with Limb Spasms after Cerebral Infarction

ZHAN Sheng, HUANG Linxing, YI Lizhen, CHEN Ruixue, HUANG Huiyuan, YUE Zenghui*

Acupuncture and Moxibustion and Rehabilitation College, Hunan University of Traditional Chinese Medicine, Changsha, Hunan 410208, China

*Correspondence: YUE Zenghui, E-mail: 624755064@qq.com

ABSTRACT Objective To observe the effect of electroacupuncture at the affected side of Quchi (LI 11) and Yanglingquan (GB 34) acupoints on cortical injury and serum inflammatory factors [interleukin-6 (IL-6) and tumor necrosis factor- α (TNF- α)], glutamate (Glu), malondialdehyde (MDA), riboflavin kinase (RFK) and NADPH oxidase 2 (NOX2) in rats with post-stroke spasticity (PSS), and to investigate the mechanism of electroacupuncture in alleviating brain injury after ischemic stroke. **Methods** A total of 30 SPF healthy adult male SD rats were randomly divided into sham operation group and model group, with 10 and 20 rats in each group. The PSS rat model was prepared by Zea-Longa suture method combined with internal capsule injection of N-methyl-D-aspartate (NMDA). After successful modeling, the model group was randomly divided into model group and electroacupuncture group, with 10 cases in each group. The rats in the model group were fixed with the rat plate without intervention, while those in the electroacupuncture group were subjected to electroacupuncture intervention. Yanglingquan (GB34, left) and Quchi (LI 11, left) acupoints on the affected side were selected, and each acupoint was directly punctured with one needle, dense wave pattern, the frequency at 100 Hz, and the intensity based on the slight shaking of rat limbs, 30 minutes a time, once a day, and the treatment lasted for 7 days. At the 1st day of modeling and the 7th day of the treatment, Zea-Longa neurological deficit score was used to assess the degree of neurological impairment. At the 2nd day of modeling and the 1st, 7th day of intervention, modified Ashworth scale (MAS) was used to assess muscle tension of the affected limbs. Hematoxylin-eosin (HE) staining was used to assess pathological changes of cerebral cortex. Enzyme-linked immunosorbent assay (ELISA) was used to detect the contents of MDA, Glu and IL-6, TNF- α in the cerebral cortex after the behavioral tests were completed. Western blot was used to analyze the protein expression level of RFK and NOX2. RT-PCR was used to analyze mRNA transcription levels of RFK and NOX2 mRNA. **Results** (1) Zea-Longa neurological deficit score and MAS score: compared with that before treatment, Zea-Longa neurological deficit score and MAS score of the electroacupuncture group decreased significantly after treatment ($P<0.05$). Compared with the sham operation group, Zea-Longa neurological deficit score and MAS score of the model group and the electroacupuncture group increased significantly after treatment ($P<0.05$). Compared with the model group, Zea-Longa neurological deficit score and MAS score of the electroacupuncture group decreased significantly after treatment ($P<0.05$). (2) Pathological changes of brain: some pathological changes(edema, hyperchromatic nuclei, irregular morphology, pyknosis, vacuolar degeneration and inflammatory cell infiltration) were observed in the model group. Compared with the model group, the pathological changes of brain tissue in the electroacupuncture group improved, the degree of neuronal injury was reduced, more normal cells were observed, the cell contour was clear, and the number of inflammatory cells decreased. (3) Contents of TNF- α , IL-6, Glu and MDA in the ischemic cortex: compared with the sham operation group, the contents of TNF- α , IL-6, Glu and MDA in the model group and the electroacupuncture group significantly increased ($P<0.05$). Compared with the model group, the contents of TNF- α , IL-6, Glu and MDA in the electroacupuncture group decreased significantly ($P<0.05$). (4) Expression level of RFK and NOX2 protein and the transcription level of RFK and NOX2 mRNA: compared with the sham operation group, expression level of RFK and NOX2 protein and the transcription level of RFK and NOX2 mRNA in the model group increased significantly after treatment ($P<0.05$). Compared with the model group, expression level of RFK and NOX2 protein and the transcription level of RFK and NOX2 mRNA in the electroacupuncture group decreased significantly after treatment ($P<0.05$). **Conclusion** Electroacupuncture can improve neurological impairment and limb spasm in rats with PSS, and its mechanism may be to the reduction down-regulation of Glu content in the cortex, reduction of the secretion of inflammatory cytokines TNF- α and IL-6, the inhibition of RFK and NOX2 expression, and the reduction of oxidative stress levels.

KEY WORDS cerebral infarction; limb spasticity; neurological impairment; oxidative stress; electroacupuncture; Quchi (LI 11) acupoint; Yanglingquan (GB34) acupoint

DOI:10.3724/SP.J.1329.2024.02006